Dalton Transactions

COMMUNICATION

View Article Online
View Journal | View Issue

Cite this: *Dalton Trans.*, 2019, **48**, 3566

Received 30th January 2019,
Accepted 18th February 2019

DOI: 10.1039/c9dt00440h

rsc.li/dalton

A decanuclear $[Dy^{III}_6Zn^{II}_4]$ cluster: a $\{Zn^{II}_4\}$ rectangle surrounding an octahedral $\{Dy^{III}_6\}$ single molecule magnet†

Nikoleta Stavgianoudaki,[a] Milosz Siczek,[b] Tadeusz Lis,[b] Giulia Lorusso,[c] Marco Evangelisti[c] and Constantinos J. Milios *[a]

An octahedral $\{Dy^{III}_6\}$ cage within a diamagnetic $\{Zn^{II}_4\}$ rectangle is reported, with magnetic relaxation studies revealing single-molecule magnet behaviour for the complex under zero external dc field with U_{eff} = 43 K and $\tau_o = 1 \times 10^{-5}$ s.

The field of lanthanide-based molecular magnetic materials has witnessed a vast growth over the last few years, due to the deeper understanding of the fundamental parameters that govern the magnetic behaviour of the 4f centres. Especially for single molecule magnets (SMMs) or single-ion magnets (SIMs), *i.e.* molecules that are able to retain their magnetism once magnetized at low temperatures upon removal of the external magnetic field,[1] employment of 4f centres has led to exceptional magnetic properties, due to both the magnitude of the spin, as well as the spin–orbit coupling based magnetic anisotropy that the 4f species possess.[2] Furthermore, for Dy-based SMMs/SIMs the uniaxial magnetic anisotropy of the Dy atoms plays a crucial role in enhancing the energy barrier, U_{eff}, needed for the re-orientation of the magnetisation, and thus molecular nanomagnets with U_{eff} values over 1000 K, and blocking temperatures as high as 60 K have been reported,[3] with the best SMM/SIM being the recently reported organometallic complex $[(Cp^{iPr5})Dy(Cp^*)]^+$ (Cp^{iPr5} = penta-iso-propylcyclopentadienyl) with an U_{eff} value of ~2210 K and a blocking temperature of ~80 K.[4] On the other hand, regarding mixed-metal 3d–4f heterometallic complexes as SMM candidates, the situation seems to differ; despite the ongoing research for the construction and characterization of 3d–4f SMMs, the energy barrier for such species remains rather low compared to 4f species, with $[Co_2Dy(L^{Br})_2(H_2O)]NO_3$ (L^{Br} = 2,2′,2″-(((nitrilotris(ethane-2,1diyl))tris(azanediyl))tris(methylene))tris-(4-bromophenol)) holding the record of U_{eff} = 600 K,[5] *i.e.* ~1/4 of the highest U_{eff} reported so far for the best lanthanide SIM/SMM. Such a discrepancy may be attributed to either weak (and most commonly antiferromagnetic) interactions between the 3d and 4f metal centres, leading to low lying split sublevels, or to the perturbation of the 4f local magnetic field due to random transversal secondary magnetic fields created by the nearby paramagnetic metal ions, resulting in quantum tunnelling of the magnetization and, thus, faster magnetic relaxation.[6]

Recently we embarked on a project of constructing heterometallic Zn^{II}–Ln^{III} clusters and investigating their magnetic properties, as a means of: (i) protecting the 4f-centres from the influence of 3d paramagnetic centres and (ii) employing a diamagnetic 3d metal atom for structural stability and diversity of the products.[7] Herein we report our latest finding regarding a decanuclear $[Zn^{II}_4Dy^{III}_6]$ complex upon employment of the Schiff-base ligand 2-(β-naphthalideneamino)-2-hydroxymethyl-1-propanol, H_3L (Scheme 1). The reaction of $Zn(OAc)_2{\cdot}2H_2O$, $Dy(NO_3)_3{\cdot}5H_2O$ and H_3L in MeOH in 1 : 1 : 1 ratio under solvothermal conditions, and in the presence of base NEt_3, gave complex $[Dy_6Zn_4O_2(L)_2(HL)_2(OAc)_8(CH_3O)_4(H_2O)_2]{\cdot}4MeOH$ (**1**·4MeOH) in good yield, which was characterized by means of X-ray single crystal crystallography.‡

[a]*Department of Chemistry, The University of Crete, Voutes 71003, Herakleion, Greece. E-mail: komil@uoc.gr*
[b]*Faculty of Chemistry, University of Wroclaw, Joliot-Curie 14, Wroclaw 50-383, Poland*
[c]*Instituto de Ciencia de Materiales de Aragón (ICMA), CSIC – Universidad de Zaragoza, 50009 Zaragoza, Spain*

† Electronic supplementary information (ESI) available: Full details of the experimental microanalyses and crystallographic data. CCDC 1892887. For ESI and crystallographic data in CIF or other electronic format see DOI: 10.1039/c9dt00440h

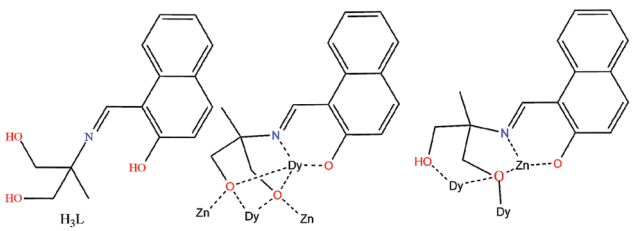

Scheme 1 The ligand and its coordination modes in **1**.

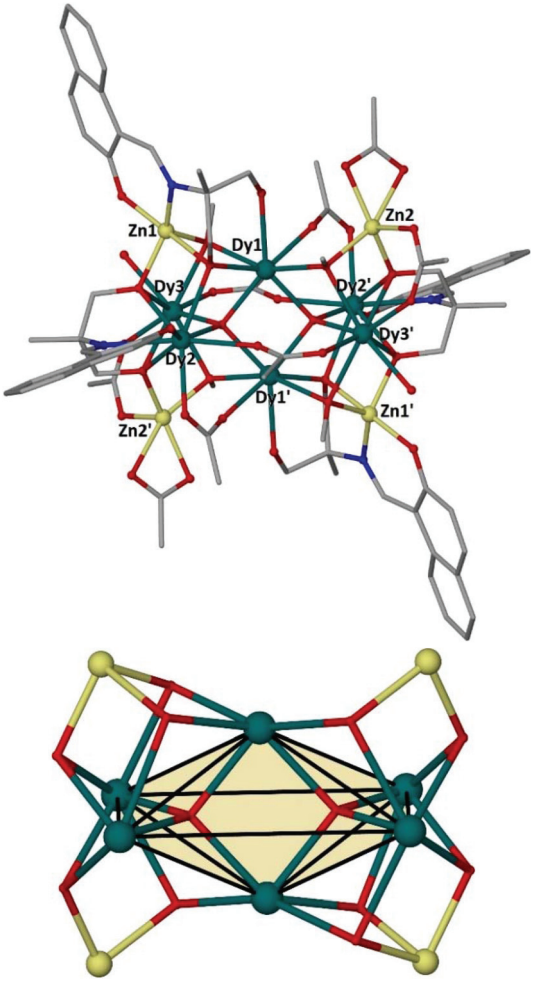

Fig. 1 The crystal structure of **1** (top) and its $\{Dy^{III}_6Zn^{II}_4\}$ metallic core (bottom) highlighting the $\{Dy^{III}_6\}$ octahedron. Colour code: Zn^{II} = yellow, Dy^{III} = dark-green, O = red, N = blue, C = grey. H-Atoms and solvate molecules are omitted for clarity.

Complex **1** crystallizes in the triclinic $P\bar{1}$ space group (Fig. 1, top). Its metallic core consists of a diamagnetic $\{Zn^{II}_4\}$ rectangular unit of ~6.12 × 6.42 Å dimensions, surrounding a central magnetic $\{Dy^{III}_6\}$ slightly "squeezed" octahedron (Fig. 1, bottom). The basal Dy^{III} ions (Dy2, Dy2′, Dy3, Dy3′) are located ~3.49 and ~5.64 Å apart, while the axial Dy^{III} centres (Dy1, Dy1′) are found ~1.73 Å above and below the basal plane.

The six metallic centres of the octahedron are held by a combination of two central μ_4-O^{2-} bridges, four monoatomic methoxide bridges, four μ–κ^1O:κ^1O' acetates and four ligands adopting two coordination modes; two of them are found in the doubly deprotonated form, HL^{2-}, with a μ_3–κ^3O:κ^1N:κ^1O':κ^1O'' coordination mode, while the remaining two are fully deprotonated, L^{3-}, adopting a μ_4–κ^3O:κ^3O':κ^1N:κ^1O'' coordination fashion. The linkage of the two metallic sub-units occurs *via* (i) the deprotonated ligands found in the molecule, (ii) the four methoxide groups, and (iii) two μ–κ^1O:κ^1O' acetate groups. Finally, two chelate acetates and two terminal water molecules fill the coordination environment of the metallic centres. All Zn centres are five-coordinate adopting square pyramidal geometry (for Zn2/Zn2′, τ = 0.160), and severely twisted square pyramidal/trigonal bipyramidal geometry (for Zn1/Zn1′, τ = 0.546). Regarding the 4f centers, their ideal geometries were found upon performing SHAPE analysis:[8] Dy2 and Dy3 are eight-coordinate with square antiprismatic (D_{4d}) geometry (SAPR-8: $S_{(\delta i,\theta i)}$ = 0.958 and $S_{(\delta i,\theta i)}$ = 1.056, for Dy2 and Dy3, respectively), while Dy1 is seven-coordinate with distorted capped trigonal prismatic geometry (C_{2v}) ($S_{(\delta i,\theta i)}$ = 11.476 for CTP) (Fig. S1 and S2†). Finally, the $\{Dy^{III}_6\}$ octahedron deviates slightly from the ideal octahedral geometry (CShM = 10.649). In the crystal lattice, the molecules pack forming layers stabilized mainly by intermolecular H-bonds between the decanuclear species and the solvate methanol molecules (Fig. 2).

DC magnetic susceptibility measurements were performed on **1** in the 2–300 K temperature range under an applied magnetic field of 0.1 T, and the results are plotted as $\chi_M T$ *vs.* T in Fig. 3, with the isothermal magnetisation (M *vs.* H) curves shown in the inset. The room-temperature $\chi_M T$ value of 81.2 $cm^3\ mol^{-1}$ K is slightly smaller than the theoretical value of 85.0 $cm^3\ mol^{-1}$ K expected for six Dy^{III} ions (S = 5/2, L = 5, J = 15/2, $^6H_{15/2}$, g_J = 4/3). Upon cooling, the $\chi_M T$ product remains practically unchanged until ~150 K, below which steadily decreases reaching 41.05 $cm^3\ mol^{-1}$ K at 2 K, possibly suggesting the presence of weak antiferromagnetic interactions within the cluster (a Curie–Weiss analysis gave θ = −2.9 K) and/or depopulation of the Dy^{III} Stark sub-levels. The isothermal magnetization *versus* B plots increase rapidly, reaching values of 29.2 and 28.5$N_{\mu B}$ at 5 T, for T = 2 and 5 K, respectively, significantly lower than the theoretical value of ~60$N_{\mu B}$ for a hexanuclear $[Dy^{III}_6]$ complex; this is mainly attributed to the presence of magnetic anisotropy and to the depopulation of the Stark sublevels.[9]

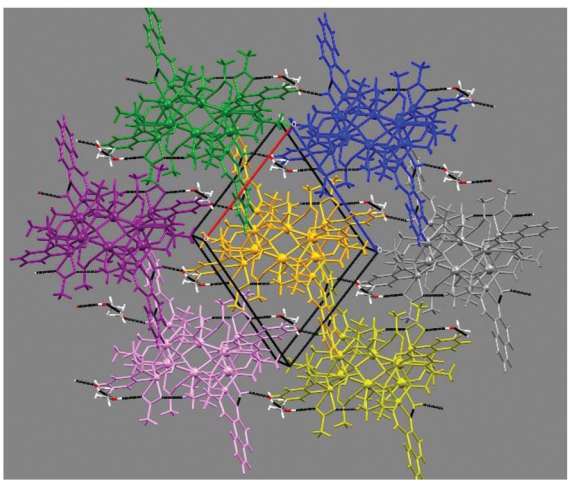

Fig. 2 Crystal packing of **1**, highlighting the intermolecular H-bonds (black bold dotted lines). Each colour corresponds to an individual molecule of **1**.

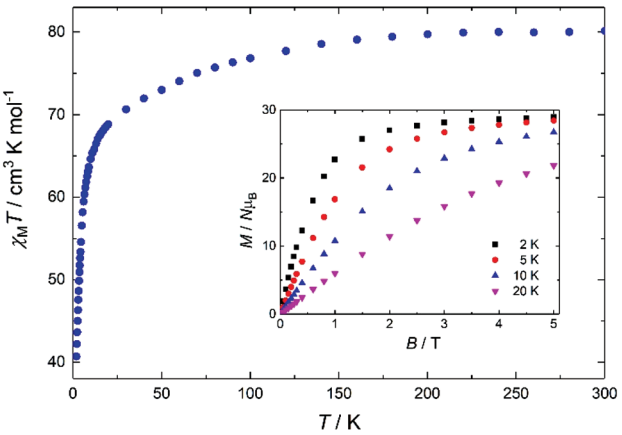

Fig. 3 Plot of $\chi_M T$ *vs.* T for **1** in the 2–300 K temperature range, under an applied field of 0.1 T. Inset: M *vs.* B for **1** in the 0–5 T and 2.0–20.0 K field and temperature ranges.

Given: (i) the large remaining magnetic moment, even at 2 K, and (ii) the square antiprismatic geometry of the Dy2 and Dy3 centres (and their symmetry related) that promotes suitable charge distribution with axial anisotropy on the Dy^{III} centres,[10] we investigated the AC dynamic magnetic properties of **1**. The measurements show temperature and frequency (f) dependent fully-formed in-phase, χ'_M, and out-of-phase, χ''_M, signals, under zero-applied DC field and a 3.5 AC field oscillating at various frequencies, in the temperature range between *ca.* 3 and 15 K (Fig. 4). This behaviour seems to indicate slow relaxation of the magnetization, which is typical for a SMM.

The main feature is a cusp in the in-phase component that occurs at approximately 10.0 K for f = 17 Hz, accompanied by a cusp in the out-of-phase component at somewhat lower temperature (Fig. 4). Effective time constants can be obtained from the reciprocal angular frequency at maximum absorption. As typical of a thermal activation process, the zero-field relaxation times so obtained can be approximated by the Arrhenius law $\tau = \tau_o \exp(U_{eff}/k_B T)$, where $\tau = (2\pi f)^{-1}$, τ_o is an attempt frequency and U_{eff} an effective energy barrier. The results are presented in the inset of Fig. 4, affording U_{eff} = 43 K and τ_o = 1×10^{-5} s. The AC susceptibility reveals that the magnetic relaxation is particularly complex in **1**, since at least another (secondary) relaxation pathway can be spotted at somewhat lower temperature than that of the main feature. In order to visualize the orientation of the anisotropy axis for each Dy^{III} ion present in **1**, we employed the electrostatic model reported by Chilton *et al.*, which is based on electrostatic energy minimization for the prediction of the ground state magnetic anisotropy axis,[11] assuming that in the absence of high symmetry the ground-state of Dy^{III} ions is a doublet along the anisotropy axis with $m_J = \pm 15/2$.[12] Following this approach, the ground state magnetic anisotropy axes in **1** were found to form three pairs from the symmetry-related Dy centres (Fig. 5); for Dy1(Dy1′) the axis is tilted towards the μ_4-O1 oxide atom, and towards O2 belonging to a monoatomic methoxide bridge and O2F belonging to bridging acetate group. For Dy2(Dy2′) the axis is pointing

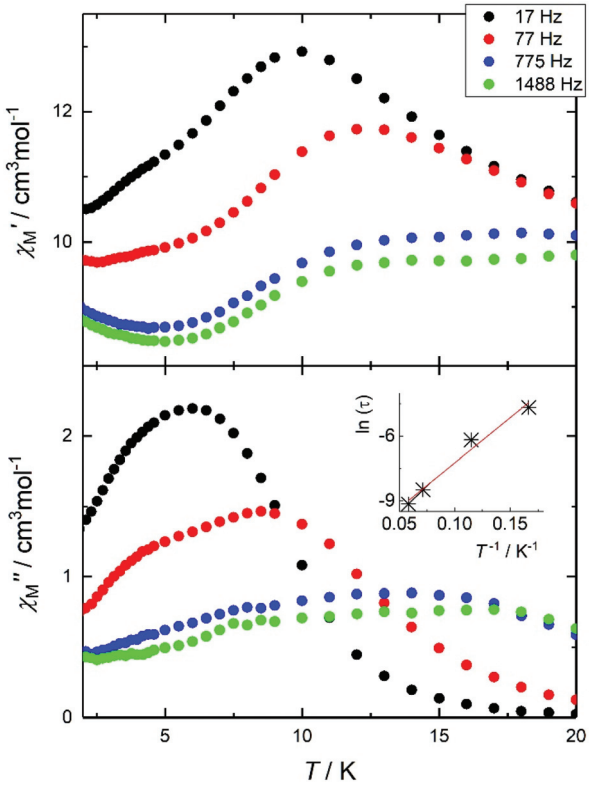

Fig. 4 (Top) In-phase, χ'_M, and out-of-phase (bottom), χ''_M, signals for **1** at various frequencies in the 17–1488 Hz range. Inset: Arrhenius fit of the effective time constants.

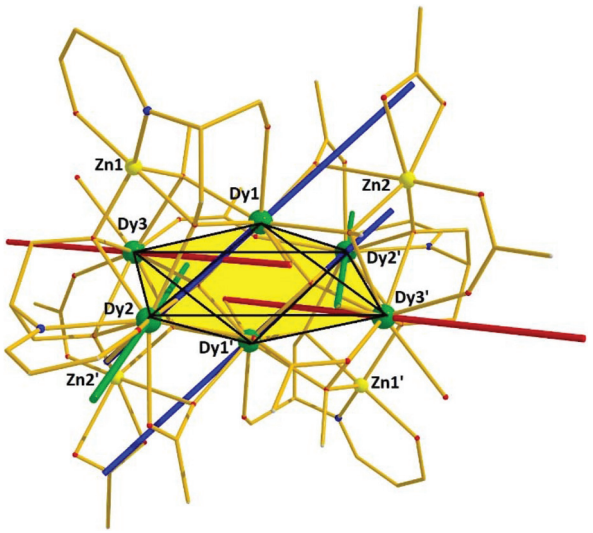

Fig. 5 Ground state magnetic anisotropy axis for the Dy centers present in **1**.

towards the μ_4-O1 oxide atom and towards O2B(O2B′) from a deprotonated aromatic hydroxyl group, while for Dy3(Dy3′) the axis is tilted towards the μ_4-O1′oxide atom and the O2D′ atom of a bridging acetate group.

Conclusions

In conclusion, in this work we present the synthesis and characterisation of a novel decanuclear $[Dy_6^{III}Zn_4^{II}]$ cluster, upon employment of the Schiff-base ligand 2-(β-naphthalideneamino)-2-hydroxymethyl-1-propanol, H_3L, with the cluster's topology describing a $\{Zn_4^{II}\}$ rectangle surrounding a $\{Dy_6^{III}\}$ octahedron. Furthermore, investigation of the magnetic properties, revealed possible SMM behaviour with U_{eff} = 43 K and $\tau_o = 1 \times 10^{-5}$ s. To the best of our knowledge, complex **1** represents the first example of a decanuclear $[Dy_6^{III}Zn_4]$ single molecule magnet.

Synthetic efforts are currently underway in order to isolate more Zn-4f clusters, as a means of investigating the effect of the diamagnetic ions on the magnetic behaviour of the 4f centres.

Conflicts of interest

The authors wish to declare no conflicts of interest.

Acknowledgements

GL and ME thank MINECO for funding (MAT2015-68204-R).

Notes and references

‡Crystal data for **1**·4MeOH: $C_{83}H_{112}Dy_6N_4O_{40}Zn_4$, M = 3042.24, triclinic, space group $P\bar{1}$, a = 13.591 (3) Å, b = 13.807 (3) Å, c = 14.560 (3) Å, α = 80.22 (2)°, β = 69.83 (2)°, γ = 77.36 (2)°, V = 2489.2 (10) Å^3, Z = 1, T = 80 K, R_1 ($I > 2\sigma$) = 0.037 and wR_2 (all data) = 0.074 for 37 200 reflections collected, 10 607 observed reflections ($I > 2\sigma(I)$) of 14 033 (R_{int} = 0.039) unique reflections and 634 parameters, GOF = 1.02. CCDC reference number: 1892887.†

1 For representative reviews on SMMs see: G. Aromi and E. K. Brechin, *Struct. Bonding*, 2006, **122**, 1; R. Bircher, G. Chaboussant, C. Dobe, H. U. Güdel, S. T. Ochsenbein, A. Sieber and O. Waldman, *Adv. Funct. Mater.*, 2006, **16**, 209; D. Gatteschi and R. Sessoli, *Angew. Chem., Int. Ed.*, 2003, **42**, 268; G. Christou, D. Gatteschi, D. N. Hendrickson and R. Sessoli, *MRS Bull.*, 2000, **25**, 66; C. J. Milios and R. E. P. Winpenny, *Struct. Bonding*, 2015, **164**, 1; L. Sorace, C. Benelli and D. Gatteschi, *Chem. Soc. Rev.*, 2011, **40**, 3092; X.-Y. Wang, C. Avendañoa and K. R. Dunbar, *Chem. Soc. Rev.*, 2011, **40**, 3213; L. R. Piquer and E. C. Sañudo, *Dalton Trans.*, 2015, **44**, 8771; R. A. Layfield, *Organometallics*, 2014, **33**, 1084; L. K. Thompson and L. N. Dawe, *Coord. Chem. Rev.*, 2015, **289**, 13; S. Demir, I.-R. Jeon, J. R. Long and T. D. Harris, *Coord. Chem. Rev.*, 2015, **289**, 149; P. Happ, C. Plenk and E. Rentschler, *Coord. Chem. Rev.*, 2015, **289**, 238; G. A. Craig and M. Murrie, *Chem. Soc. Rev.*, 2015, **44**, 2135.

2 See for example: R. Sessoli and A. K. Powell, *Coord. Chem. Rev.*, 2009, **253**, 2328; D. N. Woodruff, R. E. P. Winpenny and R. A. Layfield, *Chem. Rev.*, 2013, **113**, 5110; J. D. Rinehart and J. R. Long, *Chem. Sci.*, 2011, **2**, 2078; Y.-N. Guo, G.-F. Xu, Y. Guo and J. Tang, *Dalton Trans.*, 2011, **40**, 9953; P. Zhang, Y.-N. Guo and J. Tang, *Coord. Chem. Rev.*, 2013, **257**, 1728; Y.-N. Guo, G.-F. Xu, P. Gamez, L. Zhao, S.-Y. Lin, R. Deng, J. Tang and H.-J. Zhang, *J. Am. Chem. Soc.*, 2010, **132**, 8538; Y.-N. Guo, G.-F. Xu, W. Wernsdorfer, L. Ungur, Y. Guo, J. Tang, H.-J. Zhang, L. F. Chibotaru and A. K. Powell, *J. Am. Chem. Soc.*, 2011, **133**, 11948; B. M. Day, F.-S. Guo and R. A. Layfield, *Acc. Chem. Res.*, 2018, **51**, 1880; S. T. Liddle and J. van Slageren, *Chem. Soc. Rev.*, 2015, **44**, 6655; A. F. R. Kilpatrick, F.-S. Guo, B. M. Day, A. Mansikkamäki, R. A. Layfield and F. G. N. Cloke, *Chem. Commun.*, 2018, **54**, 7085; M. Feng and M.-L. Tong, *Chem. – Eur. J.*, 2018, **24**, 7574.

3 Y.-S. Ding, N. F. Chilton, R. E. P. Winpenny and Y.-Z. Zheng, *Angew. Chem., Int. Ed.*, 2016, **55**, 16071; D. S. Krylov, F. Liu, S. M. Avdoshenko, L. Spree, B. Weise, A. Waske, A. U. B. Wolter, B. Buechner and A. A. Popov, *Chem. Commun.*, 2017, **53**, 7901; Y.-C. Chen, J.-L. Liu, L. Ungur, J. Liu, Q.-W. Li, L.-F. Wang, Z.-P. Ni, L. F. Chibotaru, X.-M. Chen and M.-L. Tong, *J. Am. Chem. Soc.*, 2016, **138**, 2829; S. K. Gupta, T. Rajeshkumar, G. Rajaraman and R. Murugavel, *Chem. Sci.*, 2016, **7**, 5181; Y.-S. Meng, L. Xu, J. Xiong, Q. Yuan, T. Liu, B.-W. Wang and S. Gao, *Angew. Chem., Int. Ed.*, 2018, **57**, 1; A. B. Canaj, M. K. Singh, C. Wilson, G. Rajaraman and M. Murrie, *Chem. Commun.*, 2018, **54**, 8273; F.-S. Guo, B. M. Day, Y.-C. Chen, M.-L. Tong, A. Mansikkamaeki and R. A. Layfield, *Angew. Chem., Int. Ed.*, 2017, **56**, 11445; C. A. P. Goodwin, F. Ortu, D. Reta, N. F. Chilton and D. P. Mills, *Nature*, 2017, **548**, 439.

4 F.-S. Guo, B. M. Day, Y.-C. Chen, M.-L. Tong, A. Mansikkamäki and R. A. Layfield, *Science*, 2018, **362**, 1400.

5 J.-L. Liu, J.-Y. Wu, G.-Z. Huang, Y.-C. Chen, J.-H. Jia, L. Ungur, L. F. Chibotaru, X.-M. Chen and M.-L. Tong, *Sci. Rep.*, 2015, **5**, 16621.

6 M. A. Palacios, S. Titos-Padilla, J. Ruiz, J. M. Herrera, S. J. A. Pope, E. K. Brechin and E. Colacio, *Inorg. Chem.*, 2014, **53**, 1465; A. Bhunia, M. T. Gamer, L. Ungur, L. F. Chibotaru, A. K. Powell, Y. Lan, P. W. Roesky, F. Menges, C. Riehn and G. Niedner-Schatteburg, *Inorg. Chem.*, 2012, **51**, 9589.

7 N. Stavgiannoudaki, M. Siczek, T. Lis, R. Inglis and C. J. Milios, *Chem. Commun.*, 2016, **52**, 343.

8 M. Llunell, D. Casanova, J. Girera, P. Alemany and S. Alvarez, *SHAPE, version 2.0*, Barcelona, Spain, 2010.

9 J. K. Tang, I. Hewitt, N. T. Madhu, G. Chastanet, W. Wernsdorfer, C. E. Anson, C. Benelli, R. Sessoli and A. K. Powell, *Angew. Chem., Int. Ed.*, 2006, **45**, 1729; S. Osa, T. Kido, N. Matsumoto, N. Re, A. Pochaba and J. Mrozinski, *J. Am. Chem. Soc.*, 2004, **126**, 420.

10 N. Ishikawa, M. Sugita, T. Ishikawa, S.-Y. Koshihara and Y. Kaizu, *J. Am. Chem. Soc.*, 2003, **125**, 8694; M. A. AlDamen, J. M. Clemente-Juan, E. Coronado, C. Mart-Gastaldo and A. Gaita-Arino, *J. Am. Chem. Soc.*, 2008, **130**,

8874; G. Zhou, T. Han, Y.-S. Ding, N. F. Chilton and Y.-Z. Zheng, *Chem. – Eur. J.*, 2017, **23**, 1.

11 N. F. Chilton, D. Collison, E. J. L. McInnes, R. E. P. Winpenny and A. Soncini, *Nat. Commun.*, 2013, **4**, 2551.

12 See for example: S. K. Langley, N. F. Chilton, L. Ungur, B. Moubaraki, L. F. Chibotaru and K. S. Murray, *Inorg. Chem.*, 2012, **51**, 11873; G. Cucinotta, M. Perfetti, J. Luzon, M. Etienne, P.-E. Car, A. Caneschi, G. Calvez, K. Bernot and R. Sessoli, *Angew. Chem., Int. Ed.*, 2012, **51**, 1606; Y.-N. Guo, G.-F. Xu, W. Wernsdorfer, L. Ungur, Y. Guo, J. Tang, H.-J. Zhang, L. F. Chibotaru and A. K. Powell, *J. Am. Chem. Soc.*, 2011, **133**, 11948; N. F. Chilton, S. K. Langley, B. Moubaraki, A. Soncini, S. R. Batten and K. S. Murray, *Chem. Sci.*, 2013, **4**, 1719; F. Tuna, C. A. Smith, M. Bodensteiner, L. Ungur, L. F. Chibotaru, E. J. L. McInnes, R. E. P. Winpenny, D. Collison and R. A. Layfield, *Angew. Chem., Int. Ed.*, 2012, **51**, 6976.